

We are IntechOpen, the world's leading publisher of Open Access books Built by scientists, for scientists

6,900

Open access books available

185,000

International authors and editors

200M

Downloads

Our authors are among the

154

Countries delivered to

TOP 1%

most cited scientists

12.2%

Contributors from top 500 universities



WEB OF SCIENCE™

Selection of our books indexed in the Book Citation Index
in Web of Science™ Core Collection (BKCI)

Interested in publishing with us?
Contact book.department@intechopen.com

Numbers displayed above are based on latest data collected.
For more information visit www.intechopen.com



Heat Recovery and Power Generation Using Thermoelectric Generator

Luis Vitorio Gulineli Fachini, Pedro Leineker Ochoski Machado, Larissa Krambeck, Romeu Miqueias Szmoski and Thiago Antonini Alves

Abstract

In this chapter, experimental analysis of the direct conversion of thermal energy into electric energy was carried out, in order to encourage the conscious use of energy and to reduce waste. The conversion of thermal energy into electrical energy occurs in a thermoelectric generator through the Seebeck effect. This effect is associated with the appearance of an electric potential difference between two different materials, placed in contact at different temperatures. This relation between temperature and electrical properties of the material is known as thermoelectricity. This experimental study has as objective the obtaining of operating characteristic curves of the thermoelectric generator TEG1-12611-6.0, for different temperature gradients and under constant pressure between the heater plate and the heat sink. Resistors were used to heat the thermoelectric generator, which simulates the residual heat, and insulation material to minimize the dissipation of heat to the environment. For cooling, a heat exchanger was used in order to maximize the temperature difference between the sides of the thermoelectric generator. In this way, it was possible to perform an experimental analysis of the obtained electric power for different temperature ranges between the faces of the generator and, with this, verify the applicability in real systems.

Keywords: waste heat recovery, thermoelectric generator, Seebeck effect, thermal energy

1. Introduction

In 2017, total world energy consumption was approximately 13,511 million-ton equivalent of petroleum (MTEP). With the fast industrial growth of developing nations over the last decade, the industrial sector consumed approximately 2852 MTEP. It is estimated that in 2035, the world consumption of energy will increase by more than 30% [1].

Approximately 33% of the total energy consumed in the industry is rejected as residual heat, presenting as a major problem the fact that the most of this rejected energy is identified as low-quality residual heat [2]. This type of waste heat has a

small working potential, and the temperatures are below 230°C, which implies a low energy density [3]. Concurrently with the concern for global warming and the issues of diminishing oil consumption, there is a strong incentive for the development of more efficient and clean technologies for heat recovery and energy conversion systems using waste heat.

In order to minimize the waste of energy with residual heat, energy recovery systems have been more explored. These systems can become an important object of research and/or application if, at least, part of the thermal energy expelled by industrial equipment to the atmosphere can be reused [4]. In this context, experimental analysis of the direct conversion of thermal energy into electric energy, using thermoelectric generators, was carried out.

The Seebeck effect is related to the appearance of a difference of electric potential between two different materials, placed in contact, however, at different temperatures [5]. Basically, this is the same effect that occurs in thermocouples, where two different materials are connected and submitted to a temperature difference, causing a potential difference to be generated and translated into a temperature reading. In addition to this application, the thermoelectric effect can be explored in the generation of energy for wristwatches and aerospace applications or, even, in the generation of electric energy from the heated gases released in the internal combustion of engines, boiler gases, and/or the geothermal sources. The thermoelectric generators (TEG) have as main characteristics the reduced dimensions, easy adaptation in complex geometry, and very low maintenance [6]. Its conversion efficiency is about 5%; however, studies conducted at the NASA laboratory have reached 20% efficiency for high temperatures [2].

The studied thermoelectric generator consists of an arrangement of small blocks of bismuth telluride (Bi_2Te_3) doped with n -type and p -type, mounted alternately, electrically in series, and thermally in parallel between two plates of good thermal conduction [7], as shown in **Figure 1**.

The top of the p - n junction is heated, and the bottom of the set is cooled; in this way, a temperature gradient is generated. The free electrons of the n -type doped elements and the interstices of the p -type elements begin to move toward the cold part, that is, the lower part of the system. In the cold part, the n -type doped elements acquire negative polarity, while the p -type elements get positive polarity. Closing the circuit between the p - n elements, an electric potential is generated [7], and, with the electron accumulation at the cold side, an internal electric field is created, causing the Seebeck voltage.

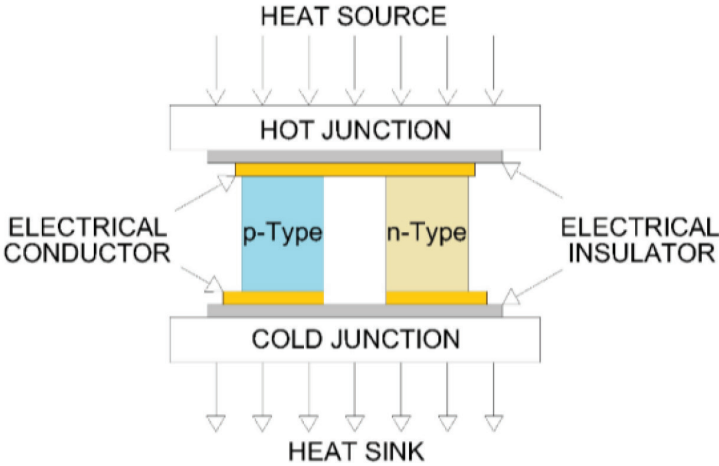


Figure 1.
Schematic diagram of a thermoelectric generator.

2. Methodology

The experimental apparatus and procedure developed for this research are described in details in this section.

2.1 Experimental apparatus

The experimental bench developed to obtain the thermoelectric generator characteristic curve, shown in **Figure 2(a)**, consisted of a laptop (*Dell*TM), an uninterruptible power supply (*NHS*TM), an aluminum block containing electrical resistors in cartridge, a thermoelectric generator (TEG1-12611-6.0), a water-cooled heat exchanger, a controlled automated resistive load variation system controlled by an *Arduino*TM, data logger (*Agilent*TM 34970A with 20 channels), a power supply unit (*Politerm*TM 16E), an ultrathermostatized bath (*SOLAB*TM SL-130), and a variable area flowmeter with throttle (*Omega Engineering*TM FL-2051). In **Figure 2(b)**, the heating and cooling system of the thermoelectric generator and the data acquisition system to obtain generated power by the thermoelectric generator TEG1-12611-6.0 are shown in detail.

The thermoelectric generator used in this experiment is made of bismuth telluride (Bi_2Te_3) and has dimensions of 56 mm by 56 mm with a height of 3.3 mm, totaling a surface area of 0.003136 m². An illustration of the generator and, also, its main specifications can be seen in **Figure 3** and **Table 1**, respectively.

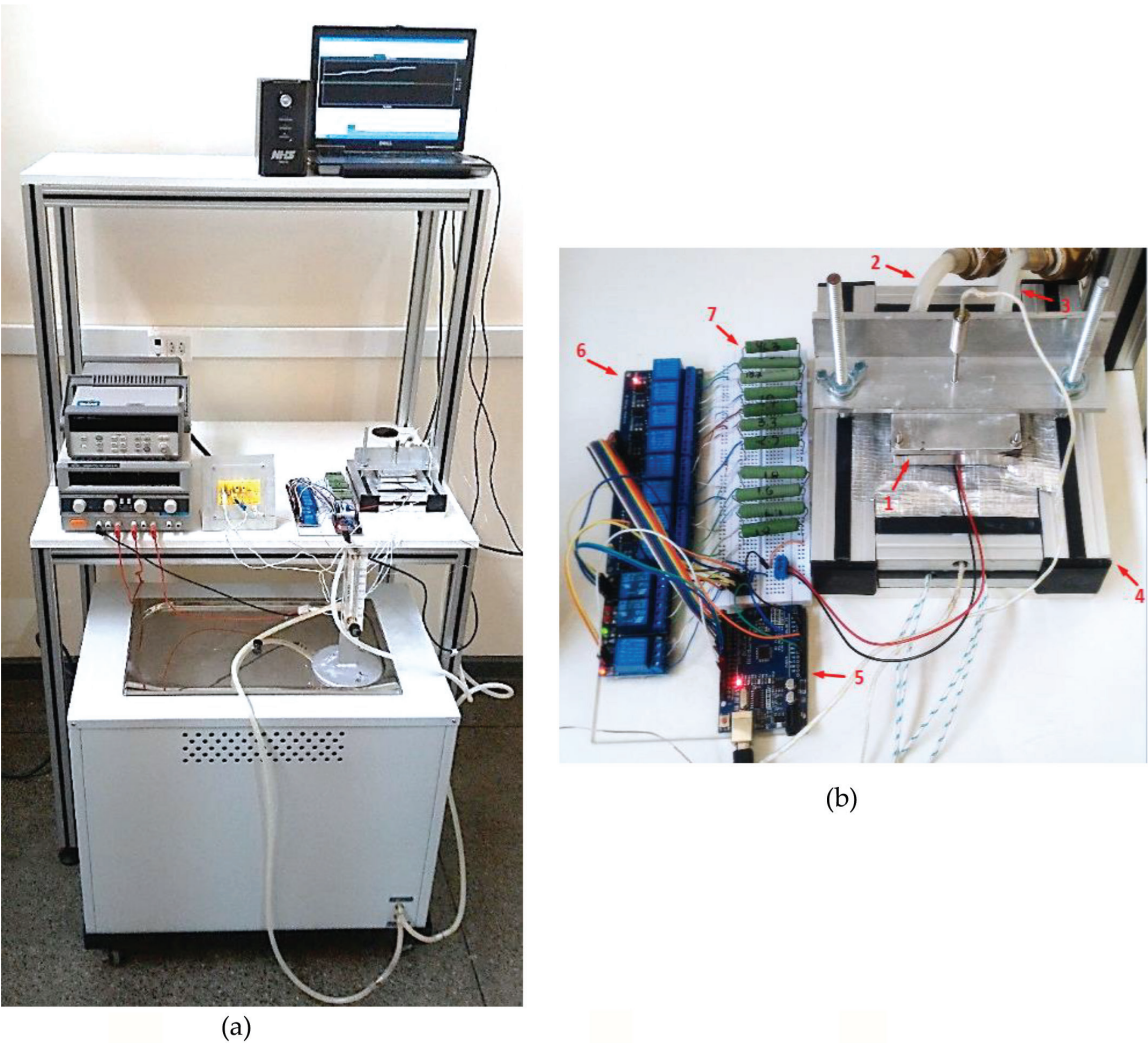


Figure 2.
Experimental apparatus. (a) Experimental bench. (b) Test section and data acquisition system.

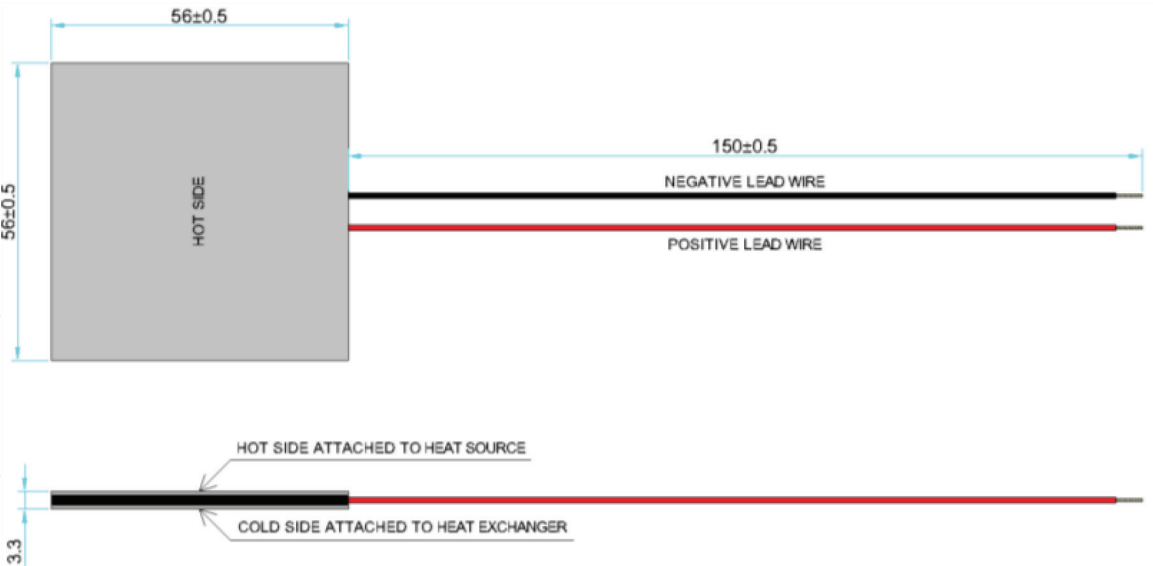


Figure 3.
Illustration of the thermoelectric generator TEG1-12611-6.0.

Parameters	Value	Unit
Hot-side temperature	300	[°C]
Cold-side temperature	30	[°C]
Open-circuit voltage	8.4	[V]
Matched load resistance	1.2	[ohms]
Matched load output voltage	4.2	[V]
Matched load output current	3.4	[A]
Matched load output power	14.6	[W]
Heat flow across the module	Approximately 365	[W]
Heat flow density	11.6	[W/cm ²]
AC resistance under 27°C at 1000 Hz	0.5 to 0.7	[ohms]

Table 1.
Main specifications of the thermoelectric generator TEG1-12611-6.0.

To measure the temperatures of the thermoelectric generator, K-type thermocouples with mineral insulation *Omega Engineering*TM, fixed inside machined channels in the heater block and the water-cooled heat exchanger, from the ultrathermostatized bath, were used. The thermocouples were positioned in order to obtain the temperatures of the heated and cooled surface of the generator (Thermocouple 1 and Thermocouple 2—**Figure 4**), resulting in the obtaining of the temperature difference between these surfaces. **Figure 4** shows the schematic diagram of the experimental system used to obtain the characteristic curve.

2.2 Experimental procedure

For the performance of the experimental tests, the ambient temperature was maintained at 16°C ± 1°C by thermal conditioning system *Carrier*TM, and the temperature of the water in the ultrathermostatized bath was also maintained at 16°C ± 1°C.

As can be seen in **Figure 4**, the thermoelectric generator was positioned between the heat exchanger and the heating system. The heat exchanger consists of an

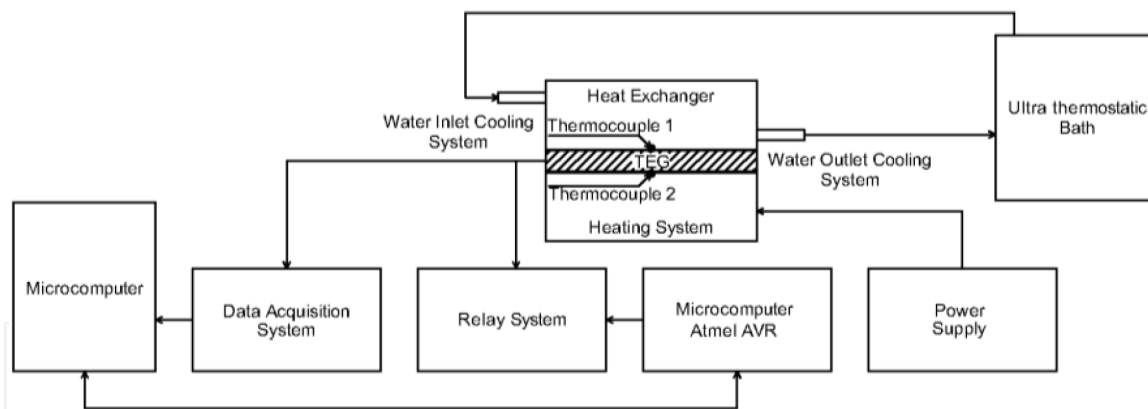


Figure 4.
 Schematic diagram of the data acquisition in the experimental apparatus.

aluminum block with machined channels inside. Water is fed by an ultrathermostatized bath with a flow rate of 1 L/min, passes through the channels in order to exchange heat with the upper surface of the TEG, and returns to the ultrathermostatized bath. The heat exchanger, the water inlet, and the water outlet in the exchanger can be observed in items (1), (2), and (3) in **Figure 2(b)**, respectively.

The heating system consists of an aluminum block located inside the base of the experimental apparatus, item (4) in **Figure 2(b)**. The block contains two cartridge resistors associated in parallel, which are responsible for the heating of the block and, consequent, the dissipation of the heat to the TEG. Each cartridge resistor has power of 200 W. In order to increase the heat exchange between the surfaces, the heating system was insulated on its sides using aeronautic thermal insulation. In addition, an aluminum bracket and two threaded rods were used to exert constant pressure in the whole system, increasing the contacts between heat exchanger - TEG and TEG - heating system. These contacts will ensure the required temperature gradient in order to get the Seebeck voltage.

The tests were performed by varying the potential difference (pd) applied to the heating system resistances, which simulate the residual heat, in order to obtain thermal loads from 40 to 320 W, with a variation of 40 W. Each thermal load was maintained for 20 minutes, where the *quasi*-permanent operating condition was reached. To ensure the data reliability, the experimental tests were repeated 3 (three) times for each dissipated power, and errors were compared taking into account that the differences between the mean values which were less than 0.5°C.

The temperature data of the hot and cold surfaces of the TEG were recorded every 10 seconds using the two thermocouples and the data acquisition system, which are saved by the software *Agilent™ Benchlink Data Logger 3*. To obtain information about the thermoelectric generator, a data acquisition system based on *Arduino™*, presented as item (5) in **Figure 2(b)**, was used. The system was responsible for switching resistive loads and obtaining values of voltage and current and, consequently, the power produced by the thermoelectric generator.

For this, an *Arduino™* programming was done to work with a set of relays and a bank of resistors, which supports up to 10 W of power, and the resistances are in a range of 1–50 Ω. In **Figure 2(b)**, the set of relays and the bank of resistors are presented as items (6) and (7), respectively. Different parallel associations between the resistors were activated, obtaining distinct loads that the thermoelectric generator was subjected. As a result, the values of voltage and current are acquired as experimental data and, consequently, the corresponding power. This system was only activated when the condition of the thermal system reached the *quasi*-permanent condition.

Parameters	Measuring instrument	Unit	Uncertainty
Input current	Power source	[A]	± 0.01
Input temperature	Ultrathermostatized bath	[°C]	± 1.00
Other temperatures	K-type thermocouple	[°C]	± 1.27
Input voltage	Power source	[V]	± 0.01
Generated voltage	Arduino™	[V]	± 0.01

Table 2.
Uncertainties of direct measurements.

Power of the power supply unit [W]	Uncertainty [W]
40	± 0.38
80	± 0.53
120	± 0.64
160	± 0.72
200	± 0.83
240	± 1.01
280	± 1.29
320	± 1.72

Table 3.
Uncertainties of indirect measurements.

2.3 Experimental uncertainties

The analysis of experimental uncertainties aims to quantify the validity of the data and their accuracy and, therefore, to allow the estimation of the random error present in the experimental results. The error is defined as the difference between the actual value and the indicated value [8].

The experimental uncertainties present in this research were associated to direct and indirect measurements, shown in **Tables 2** and **3**, respectively, and they were calculated according to the error propagation method described in [9]. The direct uncertainties are those relative to the parameters obtained using a measuring tool, being the current, input voltage and temperature, the voltage generated, and other temperatures. The uncertainty of indirect measurement is calculated in the function of other parameters, and a specific tool did not measure it. In the case of this experiment, the only indirect uncertainty is related to the power supplied by the power supply unit to the cartridge resistors, in the heating system. The power quantity was obtained by multiplying the voltage and current supplied by the source.

3. Results and discussions

First of all, the water flow through the heat exchanger, the power dissipated by the electric resistances, and the constant ambient temperature are fixed. After obtaining the *quasi*-permanent condition, the data collection and treatment were performed. **Figure 5** illustrates the output current (I_{out}) versus the output voltage (V_{out}), respectively, in [mA] and [mV], for different dissipated powers in the heating resistors.

It may be noted that the output current and voltage increase according to the temperature difference between the sides of the thermoelectric generator. It is evident from the analysis of **Figure 5** that there is high linearity obtained in the results. It may be further noted that curves have similar slopes; this means that the internal resistance of the thermoelectric generator changes minimally when the operating temperature is varied.

In **Figure 6**, for each temperature difference value, the thermoelectric generator has different internal resistance values. It is possible to note that the resistance values increase in a quadratic form with the rise of the temperature difference.

A curve adjustment with coefficient of determination (R^2) was performed close to 1. The value of the internal resistance of the generator as a function of the temperature difference (ΔT) between the sides of the thermoelectric generator can be defined by

$$Res_{int} \cong 1.092E - 3\Delta T + 0.515 \quad (1)$$

where Res_{int} is the internal resistance of the thermoelectric generator.

Therefore, the characteristic curve of the thermoelectric generator studied can be expressed by

$$U_g \cong E - (1.092E - 3\Delta T + 0.515)I \quad (2)$$

where E is the electromotive force of the electric generator, U_g is the output voltage of the generator, and I is the electric current.

Figure 7 shows the open-circuit voltage (V_{open}) and closed circuit voltage (V_{clc}) as a function of temperature differences (ΔT). The open- and closed circuit voltage increase linearly with the rise of the temperature difference. The points obtained for the closed circuit voltage are points where the maximum power generated is obtained.

The curve fit for the open-circuit voltage (U_{open}) as a function of the temperature difference (ΔT), with a determination coefficient of 0.996, can be determined by

$$U_{open} \cong 21.664\Delta T - 343.270 \quad (3)$$

where ΔT is the temperature difference between the heated and cooled surfaces of the thermoelectric generator and U_{open} is the open-circuit voltage of the generator. When the internal resistance of the generator is close to zero, it is assumed that the electromotive force of a generator is equal to the open-circuit voltage. Therefore, by substituting Eq. (3) in Eq. (2), the approximate voltage values are provided as a function of current for this thermoelectric generator, in a range of ΔT between 30°C and 230°C.

$$U_g \cong 21.660\Delta T - (1.092E - 3\Delta T + 0.515)I - 343.260 \quad (4)$$

In this way, it is possible to compare the data obtained experimentally with the theoretical values. **Figure 5** illustrates theoretical curves obtained by Eq. (4). Comparing the experimental and theoretical data, an excellent correlation between the data can be observed, showing that this equation satisfactorily represents the thermoelectric generator behavior, for a temperature difference between 30 and 230°C.

Figure 8 shows the behavior of the output power (P_{out}) as a function of the output voltage (V_{out}) parameterized in the temperature difference between the faces of the thermoelectric generator. It can be observed that with the increase in temperature difference between the faces of the thermoelectric generator, the power generated is also raised.

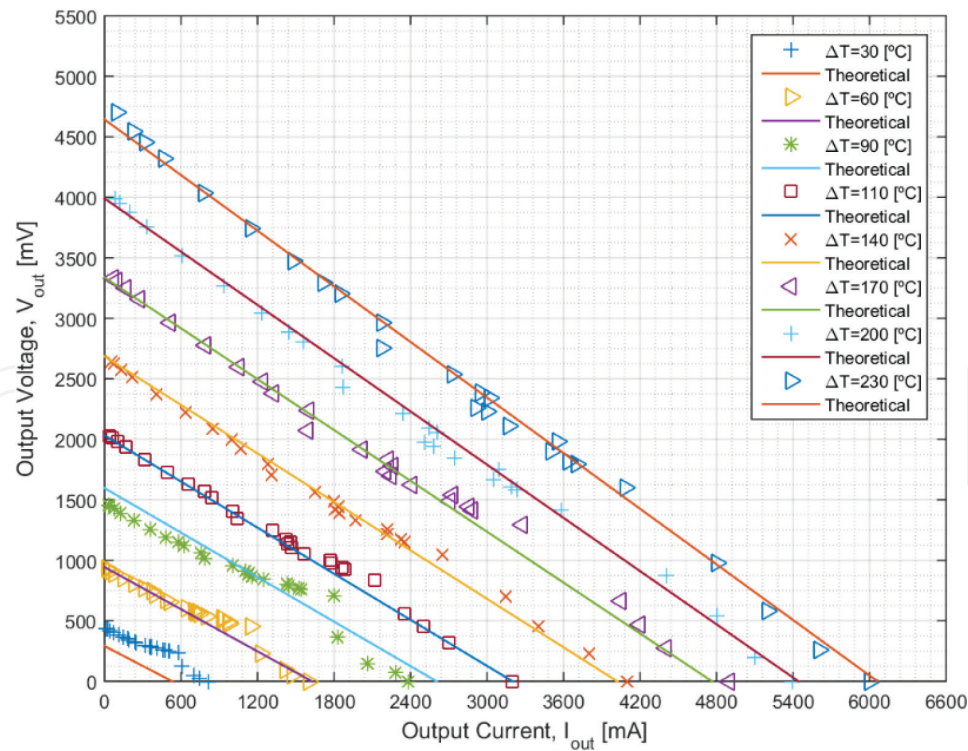


Figure 5.
Output voltage versus output current for different power dissipations.

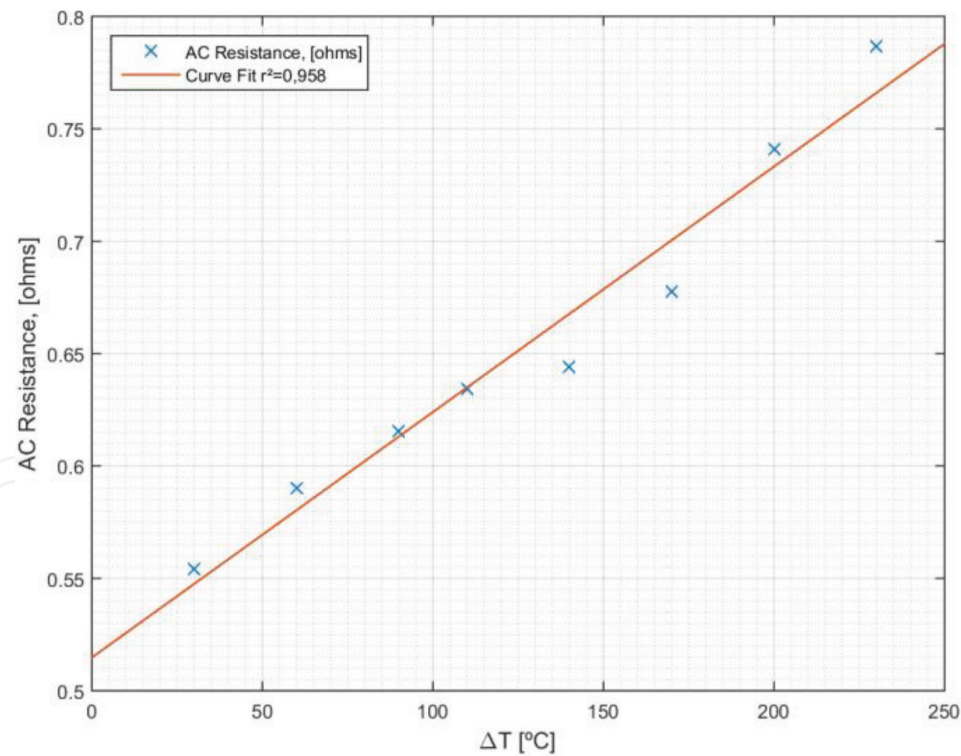


Figure 6.
Internal resistance of the thermoelectric generator.

As expected, the characteristic curves obtained follow a highly quadratic behavior, indicated by the coefficient of determination R^2 close to 1. The maximum power generated occurs when the resistance of the external load is equal to the resistance of the internal load. At this point, the power of 7068 mW is generated with a voltage of 2340 mV for the temperature difference of 230°C.

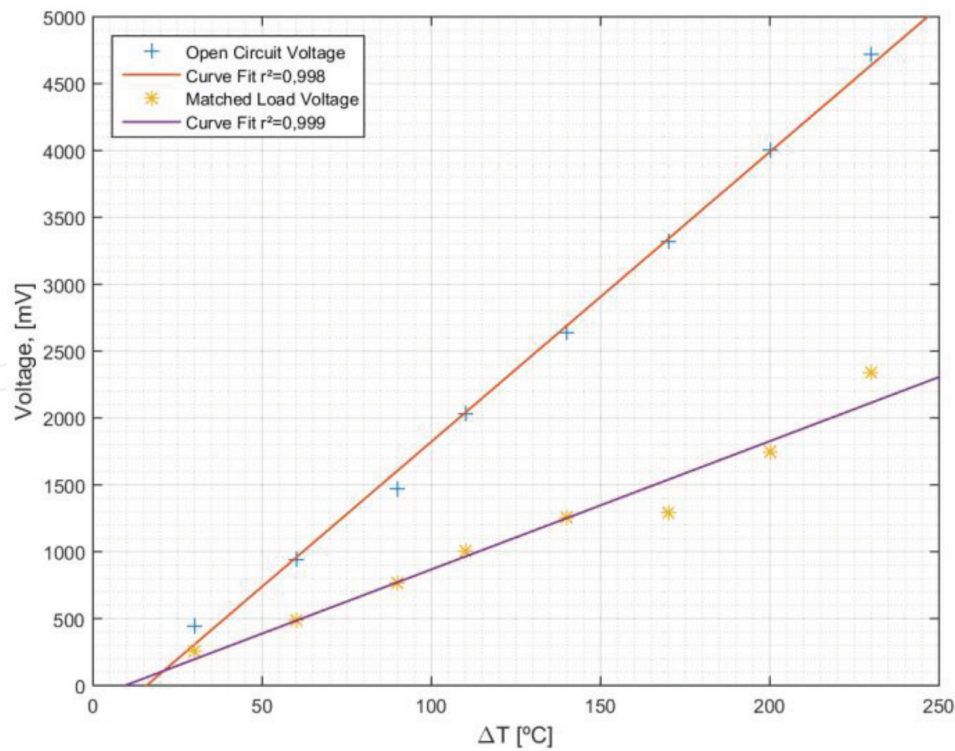


Figure 7.
Open-circuit voltage and closed circuit voltage versus temperature difference.

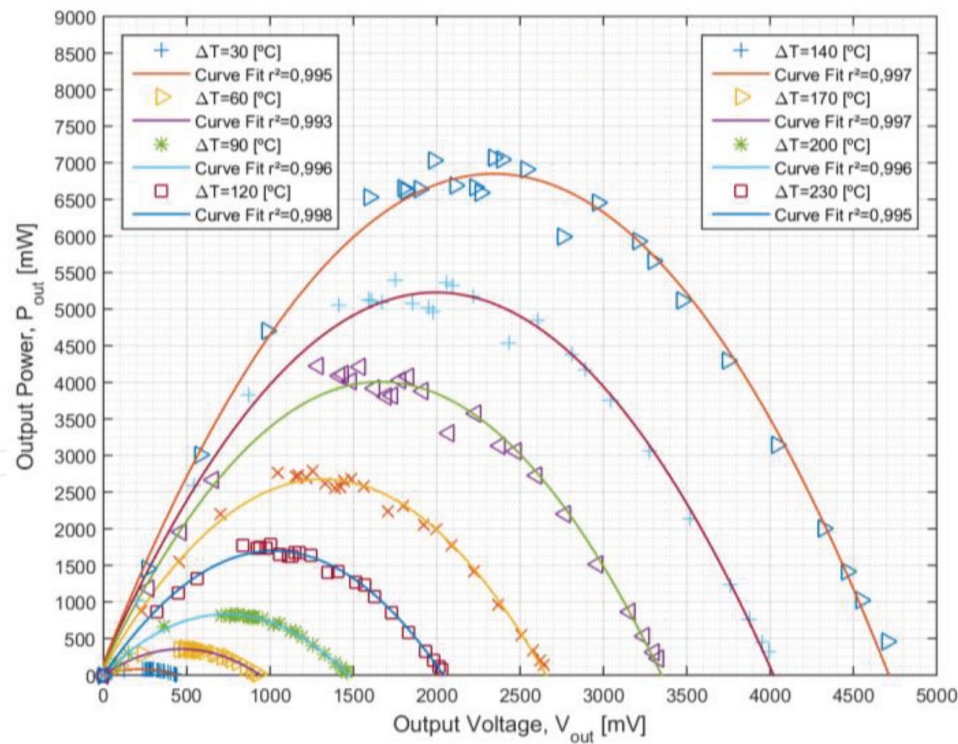


Figure 8.
Output power versus output voltage for different temperature differences.

Figure 9 indicates an alternative way to illustrate the output power data: output power (P_{out}) as a function of output current (I_{out}) parameterized in temperature differences (ΔT) between the surfaces of the thermoelectric generator. It can be seen, again, that the maximum power point is 7068 mW for a current of 3020 mA considering a temperature difference of 230°C.

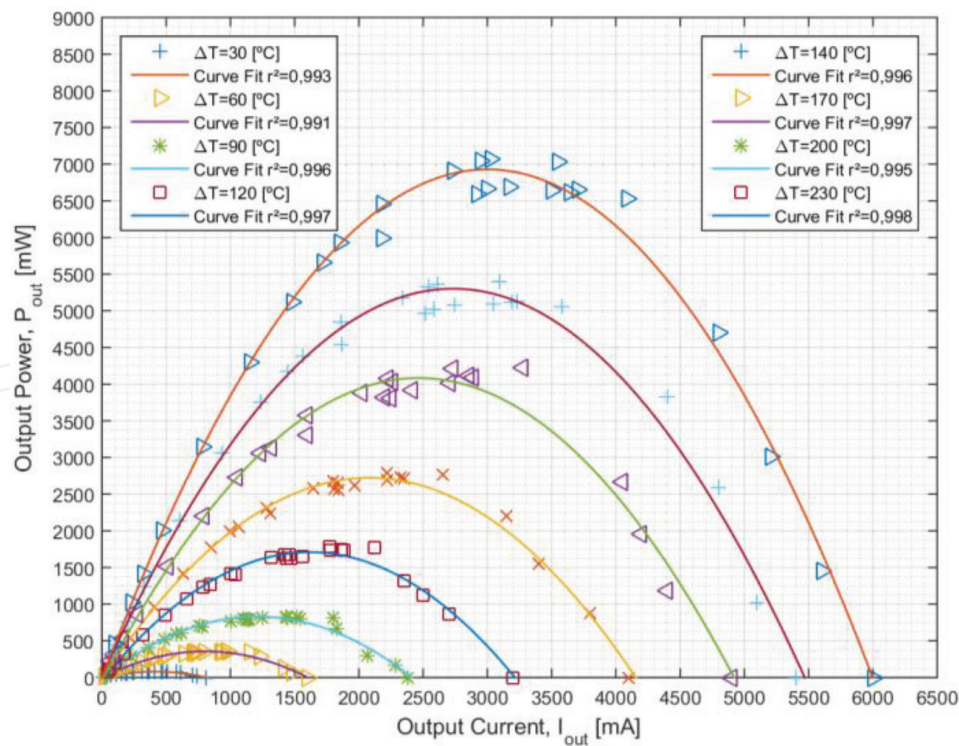


Figure 9.
Output power versus output current for different temperature differences.

Another important point to analyze is the comparison of the amount of power generated by different types of generators. For this, it is of extreme relevance to consider the size of the generators and the generated power density and not just the amount of generated power [W]. As a result, it is important to evaluate how much power is generated per square meter of the generator [W/m^2]. Thus, **Table 4** shows the power generated by the thermoelectric generator area as a function of the temperature gradient.

As shown in **Table 4**, it can be seen that in a condition such as that found in processes with residual heat release, with a temperature gradient in the range of 60°C , the thermoelectric generator is capable of generating $114.14 \text{ W}/\text{m}^2$. This value is almost the produced power by a photovoltaic solar panel of monocrystalline cells (*Siemens*TM SM46 [10]), for example, which has A-level efficiency and can generate up to $152.60 \text{ W}/\text{m}^2$. In addition, the thermoelectric generator can support higher temperature gradients and, if exposed to more extreme

Temperature difference [°C]	Generated power per area [W/m^2]
30	25.65
60	114.14
90	262.75
110	567.12
140	888.71
170	1345.38
200	1723.54
230	2253.93

Table 4.
Generated power in relation to temperature difference per area.

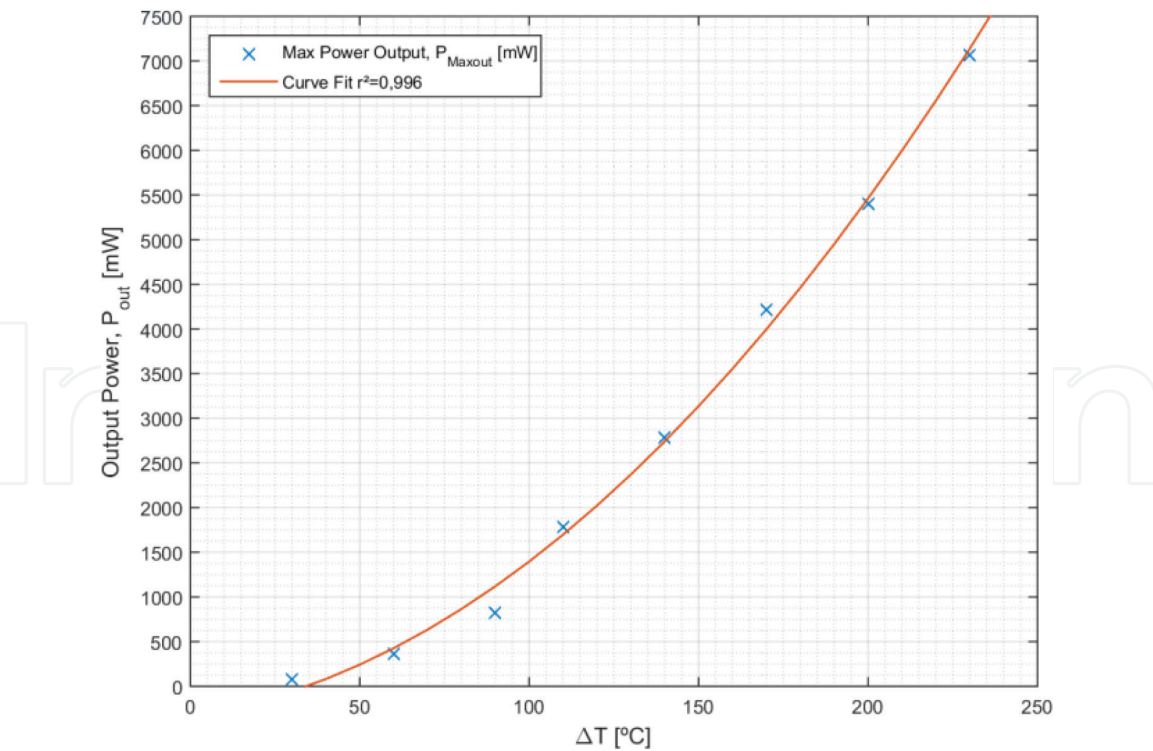


Figure 10.
Output power versus temperature difference.

conditions, can generate up to 2253.93 W/m² of electrical power for a temperature gradient of 230°C.

Figure 10 shows the behavior of the output power (P_{out}) as a function of the temperature difference (ΔT). It may be noted that with the increase in temperature difference between the surfaces of the thermoelectric generator, the power generated raises in a quadratic form.

Furthermore, the output power is limited only by the operating temperature of the thermoelectric generator, which is 270°C. Eq. (5) correlates the values of temperature difference for the electric power with a coefficient of determination of 0.996, for temperature differences greater than 7°C.

$$P_{out} = 0.117\Delta T^2 - 5.534\Delta T - 327.308 \tag{5}$$

4. Conclusions

In this chapter, experimental analysis of the direct conversion of thermal energy into electric energy was carried out. An experimental analysis was performed to obtain the operating characteristics of a thermoelectric generator of bismuth telluride (Bi₂Te₃). For this, it was necessary to develop an experimental apparatus to provide the necessary operating conditions. Therefore, it was possible to obtain the operating curves of the thermoelectric generator for a temperature difference between the surfaces of the thermoelectric generator of 30 and 230°C. It is noted that the highest power values delivered by the thermoelectric generator were for the greater temperature differences. Normalizing the power generated by the photovoltaic solar panel and the thermoelectric generator, in conditions close to the real ones of use, both have values of generated power, around 152.60 and 114.14W/m², respectively. Also, the thermoelectric generator can reach values of 2253.93 W/m² for a temperature gradient of 230°C. In conclusion, the application of thermoelectric generators in the recovery of residual heat

is a great instrument to be explored. This kind of device is compact, requires very low maintenance, and has a geometry that can be coupled in most of the industrial systems.

Acknowledgements

Acknowledgments are provided to the CAPES, the CNPq, the PROPPG/UTFPR, the DIRPPG/UTFPR, the PPGEM/UTFPR/Ponta Grossa, and the DAMEC/UTFPR/Ponta Grossa.

Nomenclature

E	electromotive force of the electric generator [mV]
I	electric current [mA]
P	power [mW]
Res	resistance of the thermoelectric generator [ohms]
R^2	coefficient of determination
ΔT	temperature difference [°C]
U	output voltage of the generator [mV]
V	voltage [mV]

Subscripts


out	output
int	internal
g	generator
opn	open circuit
clc	closed circuit

Author details

Luis Vitorio Gulineli Fachini, Pedro Leineker Ochowski Machado, Larissa Krambeck, Romeu Miqueias Szmoski and Thiago Antonini Alves*
Federal University of Technology (UTFPR), Parana, Brazil

*Address all correspondence to: thiagoaalves@utfpr.edu.br

IntechOpen

© 2019 The Author(s). Licensee IntechOpen. This chapter is distributed under the terms of the Creative Commons Attribution License (<http://creativecommons.org/licenses/by/3.0>), which permits unrestricted use, distribution, and reproduction in any medium, provided the original work is properly cited. 

References

- [1] BP. Statistical Review of World Energy June 2018. 67th ed. London, UK: BP; 2018
- [2] Fleurial JP. Thermoelectric power generation materials: Technology and application opportunities. *Journal of the Minerals, Metals and Materials Society*. 2009;**61**(4):79-85. DOI: 10.1007/s11837-009-0057-z
- [3] UNEP. Thermal Energy Equipment: Waste Heat Recovery. Energy Efficiency. 2006. Available from: www.energyefficiencyasia.org [Accessed: July 1, 2018]
- [4] Monreal J. Thermoelectrics: Material advancements and market applications [thesis]. Cambridge, US: Massachusetts Institute of Technology; 2007
- [5] Lee H. Thermal Design Heat Sinks, Thermoelectrics, Heat Pipes, Compact Heat Exchangers, and Solar Cells. New Jersey: John Wiley & Sons; 2011. 646 p
- [6] Ismail BI, Ahmed WH. Thermoelectric power generation using waste-heat energy as an alternative green technology. *Recent Patents On Electrical Engineering*. 2009;**2**:27-39
- [7] Singh BSB, Saoud A, Remeli MF, Ding LC, Date A, Akbarzadeh A. Design and construction of a simple thermoelectric generator heat exchanger for power generation from salinity gradient solar pond. *Jurnal Teknologi*. 2015;**76**(5):21-24. DOI: 10.11113/jt.v76.5527
- [8] Ismail KAR. Técnicas Experimentais em Fenômenos de Transferência. Mendes Gráfica e Editora: Campinas, BRA; 2000. 488 p
- [9] Holman JP. Experimental Methods for Engineers. 8th ed. New York, USA: McGraw-Hill; 2011. 768 p
- [10] Siemens Solar Industries. Solar module SM46. Available from: www.siemens.co.uk/sm46.html [Accessed: September 22, 2018]